Rewiring the respiratory pathway of Lactococcus lactis to enhance extracellular electron transfer

Gu, Liuyan; Xiao, Xinxin; Zhao, Ge; Kempen, Paul; Zhao, Shuangqing; Liu, Jianming; Lee, Sang Yup; Solem, Christian

Published in:
Microbial Biotechnology

Link to article, DOI:
10.1111/1751-7915.14229

Publication date:
2023

Document Version
Publisher's PDF, also known as Version of record

Received: 1 November 2022 | Accepted: 22 January 2023

DOI: 10.1111/1751-7915.14229

MICROBIAL BIOTECHNOLOGY Applied Microbiology International

RESEARCH ARTICLE

Rewiring the respiratory pathway of *Lactococcus lactis* to enhance extracellular electron transfer

Liuyan Gu[1] | Xinxin Xiao[2] | Ge Zhao[1] | Paul Kempen[3,4] | Shuangqing Zhao[1] | Jianming Liu[1] | Sang Yup Lee[5] | Christian Solem[1]

[1]National Food Institute, Technical University of Denmark, Kongens Lyngby, Denmark

[2]Department of Chemistry and Bioscience, Aalborg University, Aalborg, Denmark

[3]Department of Health Technology, Technical University of Denmark, Kongens Lyngby, Denmark

[4]National Centre for Nano Fabrication and Characterization, Technical University of Denmark, Kongens Lyngby, Denmark

[5]Department of Chemical and Biomolecular Engineering, Korea Advanced Institute of Science and Technology (KAIST), Daejeon, Republic of Korea

Correspondence
Christian Solem, National Food Institute, Technical University of Denmark, Kongens Lyngby, 2800, Denmark.
Email: chso@food.dtu.dk

Funding information
Internal PhD Scholarship of Technical University of Denmark (DTU)

Abstract

Lactococcus lactis, a lactic acid bacterium with a typical fermentative metabolism, can also use oxygen as an extracellular electron acceptor. Here we demonstrate, for the first time, that *L. lactis* blocked in NAD^+ regeneration can use the alternative electron acceptor ferricyanide to support growth. By electrochemical analysis and characterization of strains carrying mutations in the respiratory chain, we pinpoint the essential role of the NADH dehydrogenase and 2-amino-3-carboxy-1,4-naphtoquinone in extracellular electron transfer (EET) and uncover the underlying pathway systematically. Ferricyanide respiration has unexpected effects on *L. lactis*, e.g., we find that morphology is altered from the normal coccoid to a more rod shaped appearance, and that acid resistance is increased. Using adaptive laboratory evolution (ALE), we successfully enhance the capacity for EET. Whole-genome sequencing reveals the underlying reason for the observed enhanced EET capacity to be a late-stage blocking of menaquinone biosynthesis. The perspectives of the study are numerous, especially within food fermentation and microbiome engineering, where EET can help relieve oxidative stress, promote growth of oxygen sensitive microorganisms and play critical roles in shaping microbial communities.

INTRODUCTION

Lactococcus lactis is a Gram-positive lactic acid bacterium (LAB) used in various food fermentations, in particular within the dairy segment (Bourdichon et al., 2012). When grown anaerobically, NADH generated in glycolysis is re-oxidized into NAD^+ by the lactate dehydrogenase, and usually >90% of the metabolized sugar ends up as lactic acid (Figure 1A). Despite of its fermentative metabolism, *L. lactis* can be cultivated with aeration, which usually has an effect on the composition of products formed. Most *L. lactis* strains are equipped with a H_2O-forming NADH oxidase (NoxE), which uses oxygen to regenerate NAD^+ (Figure 3A), and when grown with aeration, significant amounts of acetate and acetoin are formed in addition to lactic acid (Hugenholtz et al., 2000). Furthermore, *L. lactis* has been demonstrated to have a fully functional respiratory pathway in the presence of heme, its precursor protoporphyrin IX or hemin (ferric chloride heme). *L. lactis* is equipped with type II NADH dehydrogenase (NoxAB, non-proton pumping) and a heme-dependent cytochrome *bd* oxidase and is also able to synthesize menaquinones (MK) (Figure 3A) (Pedersen et al., 2012). The cytochrome *bd* oxidase has a high affinity for oxygen and catalyses the four-electron reduction of oxygen into water (Brooijmans et al., 2007). The oxygen reduction process drives protons outside the membrane, similar to the process that occurs in a proton pump, leading to a proton motive force (PMF) across the cell membrane

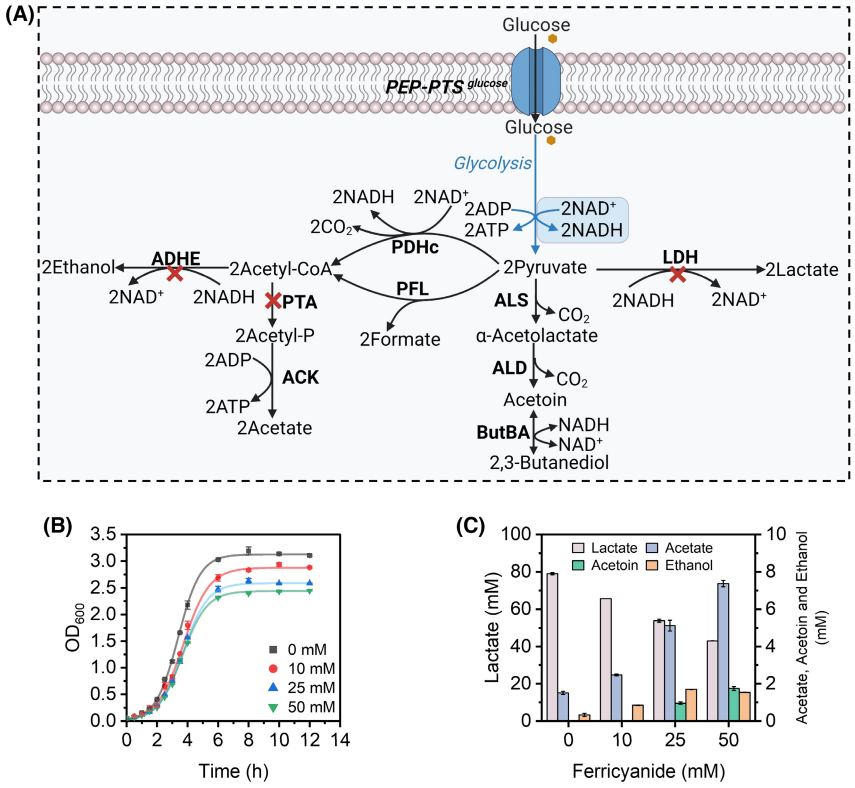

FIGURE 1 Characterization of growth and product formation of MG1363 in the presence of different concentrations of ferricyanide. (A) Schematic drawing of glycolytic pathway in *L. lactis*. LDH: lactate dehydrogenases; ALS: α-acetolactate synthase; ALD: α-acetolactate decarboxylase; ButBA: 2,3-butanediol dehydrogenase; PDHc: pyruvate dehydrogenase complex; PFL: pyruvate-formate lyase; ADHE: alcohol dehydrogenase; PTA: phosphate acetyltransferase; ACK: acetate kinase. The red crosses indicate inactivated pathways in CS4363. (B) Growth performance of MG1363 in a time course of 12 h. (C) Metabolite levels of MG1363 at the time point of 12 h. MG1363 was cultured in GM17 (M17 + Glucose) supplemented with ferricyanide under relative anaerobic conditions.

(Brooijmans et al., 2007). As a consequence, the need for proton pumping by the ATP driven F_1F_0-ATPase is reduced, which helps save ATP for growth, thereby increasing biomass yield (Koebmann et al., 2008). An additional benefit of having an active respiration is that it alleviates oxidative stress (Rezaïki et al., 2004). For these reasons, the starter culture industry frequently uses aerobic respiratory conditions when producing food cultures, and uses fish blood as a source of heme.

In food fermentations, it may be undesirable to introduce heme derived from animal blood and in particular oxygen, as oxygen is a strong oxidant that can cause lipid oxidation (Johnson & Decker, 2015) and promote unwanted microbial growth (Rodrigues et al., 2001). A promising alternative is to rely on alternative electron acceptors to oxygen for regenerating NAD^+, which has been termed extracellular electron transfer (EET) (Schröder et al., 2015). Certain microbial species, e.g., *Geobacter* and *Shewanella*, rely on EET to reduce minerals and sustain growth, which has important biotechnological applications within bioremediation and biomining. EET can also be harnessed for producing biofuels and nanomaterials (Shi et al., 2016). In recent years, EET has received increasing attention due to its important role in microbial fuel cells (MFCs), a promising technology for generating renewable bioelectricity from various biomasses (Logan, 2009). Furthermore, EET appears to play a role for growth of certain bacteria in the mammalian gut (Naradasu et al., 2019; Saunders & Newman, 2018; Wang et al., 2019). For example, the human pathogen *Listeria monocytogenes* relies on a flavin-based EET (FLEET) pathway to confer anaerobic growth advantages in the mouse intestinal lumen (Light et al., 2018). Recent studies on EET in LAB have focused on species such as *Enterococcus faecalis* (Hederstedt et al., 2020; Lam et al., 2019; Pankratova et al., 2018), *Lactiplantibacillus plantarum* (Tejedor-Sanz et al., 2022) and *L. lactis* (Freguia et al., 2009; Yamazaki et al., 2002). For the opportunistic human pathogen *E. faecalis*, it was proposed that demethylmenaquinone (DMK)-mediated EET takes place (Pankratova et al., 2018), and in this particular species a specific NADH dehydrogenase (Ndh3) and an EetA protein appear to be involved in EET (Hederstedt et al., 2020; Lam et al., 2019). In *L. plantarum*, FLEET also occurs, leading to increased NAD^+/NADH ratio and enhanced ATP formation. It has also been mentioned that *L. lactis* contains the FLEET genes except for *pplA* (Tejedor-Sanz et al., 2022). For *L. lactis*, studies have shown that EET can alter product

formation, and that the compound 2-amino-3-carboxy -1,4-naphthoquinone (ACNQ) can mediate EET when ferricyanide ($[Fe(CN)_6]^{3-}$) is used as the final electron acceptor (Yamazaki et al., 2002). ACNQ, a soluble quinone, has been shown to be endogenously produced from DHNA, a menaquinone precursor (Freguia et al., 2009). However, there are still many aspects of ACNQ-mediated EET that remain unresolved, which makes it difficult to come up with strategies to improve the capacity for EET in *L. lactis* and other LAB.

In this work, we start out by characterizing the effect of ferricyanide, a model electron acceptor in the field of bioelectrochemistry (Lai et al., 2016; Rhoads et al., 2005), on the wild-type *L. lactis* strain MG1363. Subsequently, we study how ferricyanide affects a derivative of MG1363 whose NAD^+ regeneration pathways have been partly blocked due to gene deletions in *adhE* (encoding alcohol dehydrogenase), *pta* (encoding phosphate acetyltransferase) and *ldh* (encoding lactate dehydrogenase). We substantiate that ACNQ is involved in EET and manage to enhance EET by blocking menaquinone biosynthesis. Finally, we perform adaptive laboratory evolution (ALE) to obtain mutants with enhanced EET capacity, which are characterized physiologically and by whole-genome sequencing.

EXPERIMENTAL PROCEDURES

Bacterial strains and medium

All the constructed strains and plasmids are listed in Table 1. For molecular cloning, *E. coli* strains were aerobically grown at 30°C in Luria-Bertani (LB) broth (Sigma-Aldrich, USA) supplemented with 0.2% glucose (Sigma-Aldrich, USA). *L. lactis* was cultured at 30°C in M17 broth (Thermo Fisher Scientific, USA) supplemented with 1% glucose (GM17). When required, antibiotics were added with the following concentrations: erythromycin: 200 μg/mL for *E. coli* and 5 μg/mL for *L. lactis*. 2.5 μg/mL hemin (Sigma-Aldrich, USA) was added to activate respiration.

Cultivation conditions and adaptive laboratory evolution (ALE)

In general, for growth experiments, cells from frozen glycerol stocks were streaked on GM17 agar and incubated overnight at 30°C. Single colonies were inoculated into 25 mL GM17 broth in a 300 mL shake flask aerobically at 30°C overnight to obtain the pre-culture. The pre-culture was inoculated into 2 mL fresh GM17 broth supplemented with different concentrations of ferricyanide in a 2 mL Eppendorf tube (Eppendorf, Germany) and the initial OD_{600} was 0.05. All tube cultivations were done statically (sealed tubes, no active aeration) at 30°C in an incubator.

ALE was carried out in 15 mL tubes containing 15 mL GM17 medium with 50 mM ferricyanide (Thermo Fisher Scientific, USA) under static conditions in a 30°C incubator. After reaching the stationary phase, 1.5 mL of the culture was transferred into a fresh medium. ALE of CS4363 was continued for about 6 months (approximately 600 generations). ALE of AceN was carried out for approximately 3 months.

TABLE 1 Strains and plasmids used in the study.

Name	Genotype or description	Reference
L. lactis strains		
CS4363	MG1363 Δ^3*ldh Δpta ΔadhE*	Solem et al. (2013)
CS4363-F1	CS4363 adapted on ferricyanide about 300 generations	This work
CS4363-F2	CS4363 adapted on ferricyanide about 600 generations	This work
AceN	MG1363 Δ^3*ldh Δpta ΔadhE ΔbutBA ΔnoxE*	Liu et al. (2017)
AceN-F	AceN adapted on ferricyanide	This work
CS4363-MA	MG1363 Δ^3*ldh Δpta ΔadhE ΔmenA*	This work
CS4363-MB	MG1363 Δ^3*ldh Δpta ΔadhE ΔmenB*	This work
CS4363-NAB	MG1363 Δ^3*ldh Δpta ΔadhE ΔnoxAB*	This work
CS4363-UE	MG1363 Δ^3*ldh Δpta ΔadhE ΔubiE*	This work
Plasmids		
pCS1966	*oroP*-based selection/counters election vector, Em^R	Solem et al. (2008)
pCS1966menA	Plasmid used for deleting *menA*	This work
pCS1966menB	Plasmid used for deleting *menB*	This work
pCS1966noxAB	Plasmid used for deleting *noxAB*	This work
pCS1966ubiE	Plasmid used for deleting *ubiE*	This work

DNA techniques

To prepare electrocompetent cells of *L. lactis*, cells were grown in GM17 to OD_{600} of 0.5 to 0.8 and then inoculated (1%) into 25 mL GM17 containing 0.5 M sucrose (SGM17) supplemented with 1% glycine. The cells were harvested at OD_{600} of 0.2 to 0.7 by centrifugation at 4°C, 4000 × *g* for 10 min. After washing twice in ice-cold 0.5 M sucrose containing 10% glycerol, the cells were suspended in 250 μL washing solution and the solution was divided into small portions by 50 μL. Then the cells were stored at −80°C until use (Holo & Nes, 1989). One shot™ top10 chemically competent *E. coli* (Thermo Fisher Scientific, USA) was used for storing recombinant plasmids. Phusion high-fidelity DNA polymerase (Thermo Fisher Scientific, USA) was used for PCR amplification. Gibson assembly HiFi master mix (Thermo Fisher Scientific, USA) was used for assembling gene fragments. DreamTaq Hot Start DNA polymerase (Thermo Fisher Scientific, USA) was used for PCR verification. Monarch plasmid miniprep kit (New England Biolabs, USA) was used for plasmid extraction from *E. coli*. The DNA sequencing was performed by Macrogen (South Korea).

Construction of knock-out plasmids and strains

PCR primers used are shown in Table S1. The plasmid pCS1966 was used for knocking out genes in *L. lactis* (Solem et al., 2008) and detailed sequence of multiple cloning site (MCS) of it can be found in Figure S5. Derivatives of pCS1966 for deleting *menA*, *menB*, *noxAB* and *ubiE* were constructed as described below. When constructing knock-out plasmids: pCS1966menA, pCS1966menB, pCS1966noxAB and pCS1966ubiE, ~1000 bp regions upstream and downstream of the deleted genes were amplified by Phusion high-fidelity DNA polymerase. The primers used for amplifying upstream and downstream of the deleted genes: 2-up-F/R (*menA-upstream*), 3-up-F/R (*menB-upstream*), 4-up-F/R (*noxAB-upstream*), 7-up-F/R (*ubiE-upstream*), 2-down-F/R (*menA-downstream*), 3-down-F/R (*menB-downstream*), 4-down-F/R (*noxAB-downstream*) and 7-down-F/R (*ubiE-downstream*). Phusion high-fidelity DNA polymerase was also used to generate linearized versions of plasmid pCS1966. Primers 2-plas-F/R, 3-plas-F/R, 4-plas-F/R and 7-plas-F/R were used for corresponding genes. To insert upstream and downstream sequence in MCS of pCS1966, upstream, downstream and linearized plasmid were assembled by using the Gibson assembly HiFi master mix. The recombinant plasmids were introduced into prepared *L. lactis* competent cells by electroporation using a MicroPulser Electroporator (Bio-Rad, Hercules, USA). The electroporation condition: voltage 2.0 kV, resistance 200 Ω and time constants of 4.5 to 5 ms (Holo & Nes, 1989). The successful integration resulted in erythromycin resistance. 5-fluoroorotic acid (Thermo Fisher Scientific, USA) was used for the counter selection (Solem et al., 2008). Deletions were verified using primers 2-F/R (*menA*), 3-F/R (*menB*), 4--F/R (*noxAB*) and 7-F/R (*ubiE*) with DreamTaq Hot Start DNA polymerase. The PCR sequences are provided in Table S3.

Measurement of cell growth

Cell growth was measured by recording the time profile of optical density at 600 nm (OD_{600}). Since the medium changed colour during growth, cells were harvested by centrifugation (14,000 rpm, 2 min), washed and resuspended in dH_2O prior to measurements. dH_2O was used as reference. Specific growth rates were calculated as described by Widdel (2010).

Quantification of fermentation metabolites

Quantification of metabolites (glucose, pyruvate, acetoin, 2,3-butanediol) was carried out by high-performance liquid chromatography (HPLC) using an Aminex HPX-87H column (Bio-Rad, Hercules, USA). 5 mM H_2SO_4 was used as the mobile phase at a flow rate of 0.5 mL/min. The temperature of the column oven was set to 60°C. Glucose, acetoin, and 2,3-butanediol were quantified using an RI detector, while pyruvate was quantified using a UV detector at the wavelength of 210 nm. The samples for HPLC analysis were filtered using 0.22 μM filters (Labsolute) immediately after sampling and were stored at −20°C.

Quantification of ACNQ and DHNA

Quantification of ACNQ and DHNA was carried out by HPLC equipped with the HC-C18 column (Agilent, USA). ACNQ standard (ALB Technology, Hong Kong) and DHNA standard (Sigma-Aldrich, USA) were used to prepare standard curves. The mobile phase was a 23:77 mixture of acetonitrile and 0.2% acetic acid, respectively. The temperature of the column oven was set at 40°C and the flow rate was 0.5 mL/min. The concentration of ACNQ and DHNA was measured using UV detector at the wavelength of 269 nm.

Determination of pH change

An iCinac instrument (KPM Analytics, USA) was used to determine pH profiles. The overnight seed culture was inoculated in fresh GM17 medium with different

concentrations of ferricyanide to reach an initial OD_{600} of 0.05. The total volume was set to 40 mL in a 50 mL centrifuge tube. After inserting the pH-electrode the tube was almost completely filled. The tubes were sealed with sterilized laboratory wrapping film (parafilm, Bemis, USA). The centrifuge tubes were placed in a 30°C water bath. Immediately after the addition of the cells, pH recording was initiated.

Measurement of NADH/NAD^+ ratio

Samples were taken from exponentially growing cultures of *L. lactis*. Then samples were rapidly chilled down by centrifugation at 4°C, 14,000 rpm for 2 min and the supernatants were discarded. The pellets were quenched quickly with liquid nitrogen and subsequently stored at −20°C before measuring. The extraction and quantification of NADH/NAD^+ were performed using the NAD^+/NADH-Glo™ Assay kit (Promega, Madison), following the instructions from the supplier. The cell dry weight (CDW) was calculated by using equation: CDW (g/L) = 0.37 g/L × OD_{600} (Lan et al., 2006).

Scanning electron microscopy (SEM) of cell morphology

CS4363 cells were cultured with/without ferricyanide until the stationary phase. Then cells were collected by centrifugation and the supernatants were removed. The pellets were washed and re-suspended in 100 mM phosphate-buffered saline (PBS) buffer (pH 7.4). An equal volume of fixative, consisting of 4% glutaraldehyde and 8% paraformaldehyde in water, was added to the cell suspension and maintained at room temperature for 1 h. After that, the samples were kept at 4°C until imaging. The morphology was observed by using 5 kV in an FEI Quanta FEG 200 Environmental SEM.

Wavelength scan and detection of ferricyanide and ferrocyanide

Wavelength scan of 100 μL 8 mM ferricyanide (dissolved in GM17), 8 mM ferricyanide (dissolved in GM17), and empty GM17 medium separately were conducted by Infinite 200 PRO microplate reader (Tecan, Switzerland). The range of wavelength scan was from 315 to 500 nm. The calibration curve of ferricyanide and ferrocyanide was measured at 420 nm and at 320 nm, respectively. The supernatant of sample was obtained by centrifugation and 100 μL was taken for measurement at 420 and 320 nm. The detailed calculation process can be found in Figure S1.

Electrochemical measurements

Cyclic voltammetry (CV) was recorded by using a potentiostat (Autolab PGSTAT12, EcoChemie, Netherlands) in a three-electrode setup, using a Ag/AgCl with saturated KCl as the reference electrode, a platinum wire counter electrode, and a glassy carbon working electrodes (GCE, diameter: 0.4 cm) respectively. CVs were usually recorded with a scan rate of 5 mV/s. For CVs of ACNQ, menadione and ferricyanide, different scan rates of 5, 20, 50, 100 and 200 mV/s were used. Before electrochemical measurements, GCEs were polished with 0.1 and 0.05 μm Al_2O_3 slurries sequentially. Then GCEs were sonicated in acetone for 5 min twice and subsequently in deionized water for 5 min. The electrolyte was GM17 medium. Dissolved oxygen was removed by bubbling argon gas through the medium and argon was maintained above the solution throughout the measurements.

Recovery test of EET ability in knock-out strain CS4363-MB

Overnight pre-cultures of CS4363-MB were inoculated into 2 mL fresh GM17 broth with 50 mM ferricyanide supplemented with different concentrations of DHNA (0.01–0.2 mM), ACNQ (0.01–0.2 mM), menadione (0.05–1 mM) and menaquinone-4 (MK-4) (0.1–1 mM), respectively, in 2 mL Eppendorf tubes and the initial OD_{600} was 0.05. DHNA and ACNQ were dissolved in methanol. Menadione and MK-4 were dissolved in ethanol. Considering that organic solvents may have a negative effect on the growth of the cell, cultures containing the equivalent volume of methanol and ethanol were included as well. The relative OD_{600} = OD_{600} (add ACNQ/DHNA/menadione/MK-4) – OD_{600} (add same volume of methanol/ethanol) was adopted. The samples at 0 and 12 h were taken for further HPLC analysis.

Complementation assays for multiple strains

Overnight cultures of CS4363, CS4363-MA, and CS4363-MB were streaked on GM17 supplemented with 50 mM ferricyanide using sterile loops. After the plates had been dried on a flow clean bench, they were incubated overnight in the anaerobic tank with an anaerobic bag. Digital photos were taken of plates placed on a lightbox.

Whole genome sequencing

Whole genome sequencing of CS4363, AceN, CS4363-F1, CS4363-F2, and AceN-F was carried out

by BGI Europe A/S (Denmark), using PE150 sequencing and the DNBseq tech platform (BGISEQ) (Zhou et al., 2019). After the preparation of short insert fragment library preparation, at least 1Gb data per sample was generated. Geneious Prime (Auckland, New Zealand) was used to analyse the sequencing data, map the genome, and identify variations. The *L. lactis* MG1363 (Genbank accession number: NC009004) genome was used as a reference. Single nucleotide variations (SNVs) were identified based on Bowtie2 assembled data. The SNVs were compared between all ferricyanide adaptive strains and their parental strains. The genome sequencing project has been deposited in the NCBI under the BioProject (https://www.ncbi.nlm.nih.gov/bioproject) accession PRJNA869519. The sequencing data have been deposited in NCBI Sequence Read Archive (SRA; https://www.ncbi.nlm.nih.gov/sra) under the accession numbers of SRR21065319, SRR21065318, SRR21065317, SRR21065316, and SRR21065315.

RESULTS

Growth and product formation of wild-type *L. lactis* is perturbed by ferricyanide

Ferricyanide is chosen as a model electron acceptor due to its relatively moderate redox potential, which is insensitive to pH changes in the media (Yan et al., 2021). It can serve as an excellent electron acceptor in EET (Ucar et al., 2017), but has also been reported to be toxic to certain bacteria (Liu et al., 2009). To determine how *L. lactis* responds to the presence of ferricyanide, we grew the wild-type *L. lactis* MG1363 in rich GM17 medium containing different amounts of ferricyanide. As shown in Figure 1B, the growth of MG1363 was somewhat inhibited by ferricyanide, and the specific growth rate decreased to $0.870 \pm 0.006\,h^{-1}$ in the presence of 50 mM ferricyanide, which was 22% below that of MG1363 without ferricyanide. The effect of ferricyanide was directly correlated to the concentration (Figure 1B). Ferricyanide also altered fermentation product composition and promoted the formation of acetate, ethanol and acetoin (Figure 1C), suggesting that ferricyanide indeed was involved in NAD^+ regeneration and EET.

Extracellular electron transfer enables growth of an *L. lactis* mutant partly blocked in NAD^+ re-generation

CS4363, a derivative of MG1363, which is partly blocked in NAD^+ regeneration, is unable to grow under strictly anaerobic condition. However, it can grow under aerated conditions where oxygen serves as electron acceptor (Liu et al., 2017; Solem et al., 2013) (Figure 1A). Based on the observations with the wild-type strain MG1363, we speculated that CS4363 might be able to grow under anaerobic (or O_2-limiting) conditions in the presence of ferricyanide, and this was indeed what we found. As the concentration of ferricyanide increased from 25 to 150 mM, the time to reach the stationary phase was shortened from 12 to 8 h (Figure 2A). Without ferricyanide added, limited growth was observed, which was due to small amounts of dissolved oxygen in the medium. At the highest concentration tested (150 mM), the specific growth rate of CS4363 was $0.626 \pm 0.009\,h^{-1}$. The final OD_{600} reached around

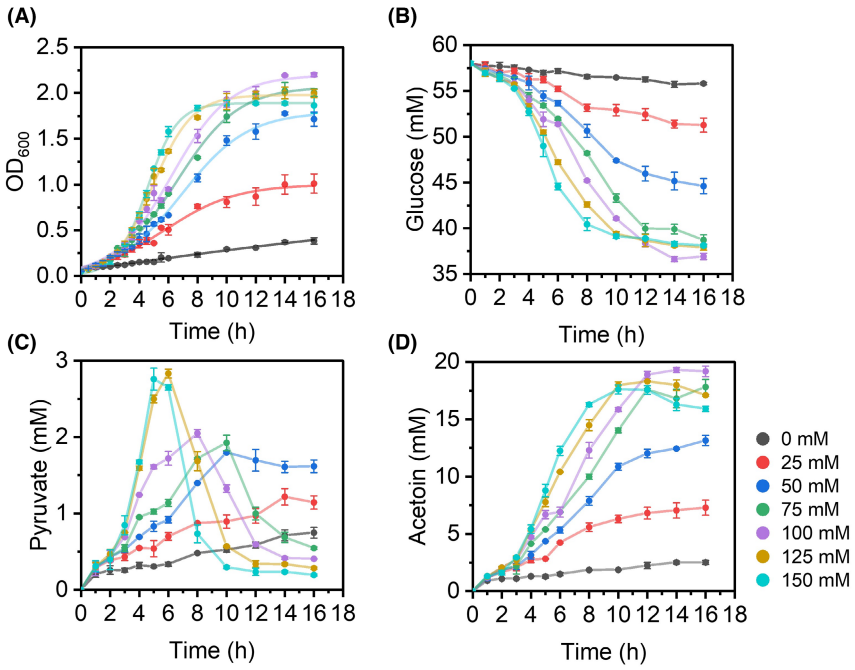

FIGURE 2 Characterization of growth and product formation of CS4363 in the presence of different concentrations of ferricyanide. (A) Time profiles of growth performance. (B) Glucose consumption. (C) Pyruvate formation. (D) Acetoin formation. CS4363 was cultured in GM17 supplemented with ferricyanide under relative anaerobic conditions.

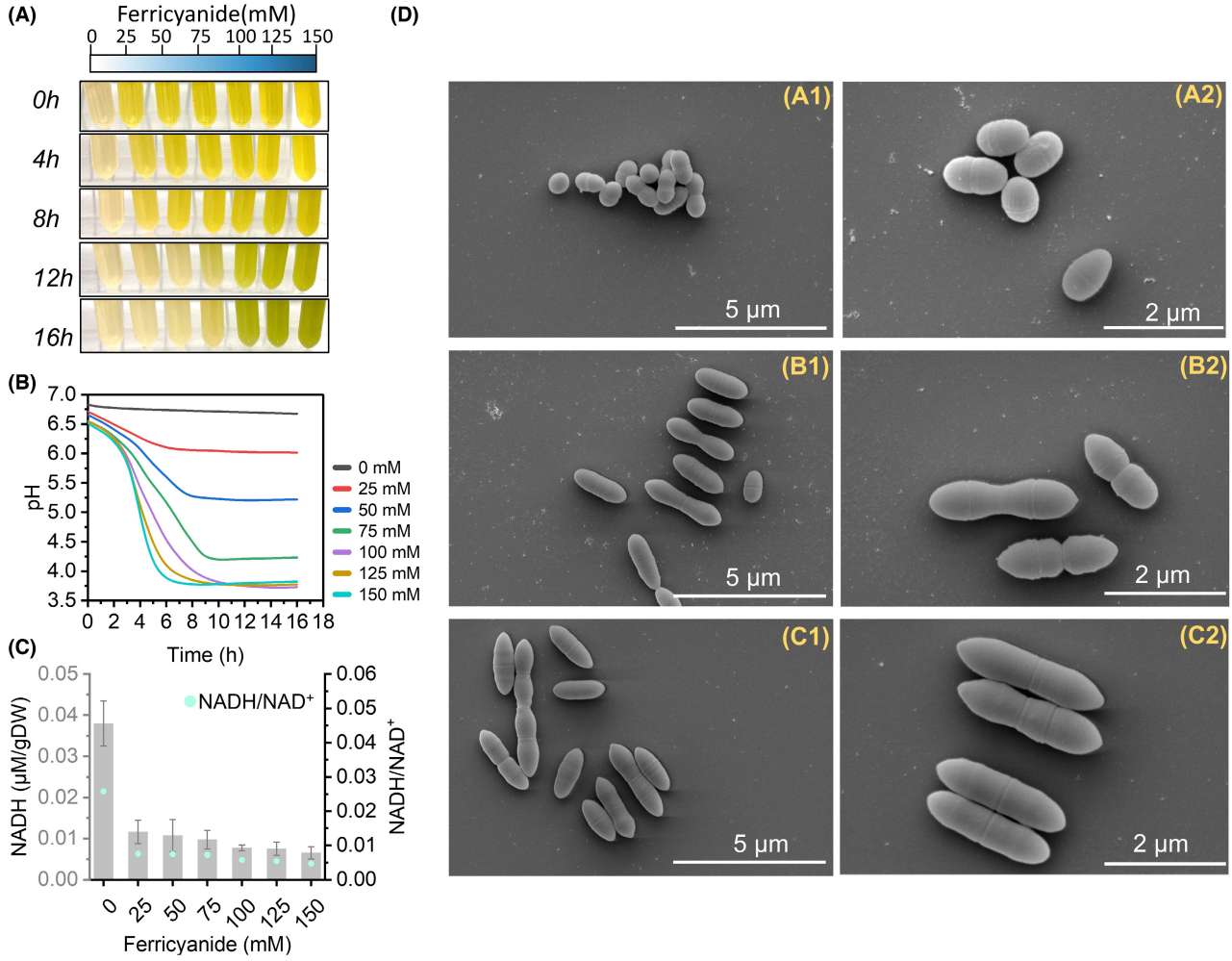

FIGURE 3 The concentration effect of ferricyanide on CS4363. (A) The colour change with time at different concentrations of ferricyanide. (B) The pH change with time at different concentrations of ferricyanide. (C) NADH/NAD$^+$ ratio changes at different concentrations of ferricyanide at exponential phase. (D) SEM images of CS4363 at stationary phase without ferricyanide (A1, A2), with 50 mM ferricyanide (B1, B2) and 150 mM ferricyanide (C1, C2). CS4363 was cultured in GM17 supplemented with ferricyanide under relative anaerobic conditions.

2 when the concentration of ferricyanide was in the range 75 to 150 mM, and a similar amount of glucose had been consumed by these cultures (Figure 2B). For all ferricyanide concentrations tested, a small amount of pyruvate was detected, the concentration of which peaked in the late exponential phase and subsequently declined; there was a clear correlation between pyruvate production and ferricyanide concentration (Figure 2C). In conclusion, ferricyanide enabled anaerobic growth of CS4363 with acetoin as the main fermentation product (Figure 2D).

As CS4363 grew in the medium containing ferricyanide, the colour changed due to the reduction of ferricyanide (yellow) to ferrocyanide (colourless) (Figure 3A). At higher concentrations, exceeding 75 mM, the colour of the medium became greenish after 12 h, and the pH dropped to approximately 3.8 ± 0.0 in 16 h (Figure 3B). It has been reported that, ferricyanide can decompose in acidic media (pH < 4.0), generating free iron species and finally Prussian blue ($Fe_4[Fe(CN)_6]_3$) (Domingo et al., 1990; Husmann et al., 2020), which may explain the observed green colour. The concentration of ferricyanide and ferrocyanide was quantified by an optical method described by Lai et al. (2016) (Figure S1A–D). As shown in Figure S1E,F, for CS4363, when grown in the presence of 25 or 50 mM ferricyanide, ferricyanide was stoichiometrically reduced to ferrocyanide at 16 h. At ferricyanide concentrations above 75 mM, part of the ferricyanide appeared to decompose into Prussian blue due to the acidic pH, which has been reported previously (Husmann et al., 2020) (Figure 3B).

As can be seen in Figure 3B, the pH of the culture medium dropped more quickly with increasing concentrations of ferricyanide, implying that NADH was oxidized more rapidly to NAD$^+$ thereby leading to quicker acidification of the medium. This could also be seen directly from the trend of the NADH/NAD$^+$ ratio measured, which decreased from 0.0258 ± 0.0002 (without

ferricyanide) to 0.0047 ± 0.0011 (with 150 mM ferricyanide) (Figure 3C). Besides its growth stimulating effect on CS4363, ferricyanide also had a clear effect on cell morphology (Figure 3D), and with increasing ferricyanide concentrations the cells became more rod-shaped.

Blocking menaquinone biosynthesis can enhance EET in *L. lactis*

The role of diaphorase and ACNQ for EET in *L. lactis* has been indicated previously (Yamazaki et al., 2002). NADH dehydrogenase (NoxAB) is an example of a diaphorase (Collins et al., 2016). ACNQ was identified to be a soluble analog of menaquinone (MK), which is derived from 1,4-dihydroxy-2-naphthoic acid (DHNA), an intermediary in menaquinone biosynthesis, formed without the participation of enzymes (Mevers et al., 2019). As shown in Figure 5A, the menaquinone biosynthesis pathway can be divided into two parts: production of the napthoate ring: DHNA and production of the polyprenyl diphosphate (PPP) chain. The precursors D -erythrose-4-phosphate (E4P) and phosphoenolpyruvate (PEP) are converted to DHNA by shikimate and menaquinone pathways. Acetyl-CoA from glycolysis is converted to PPP chain by mevalonate and polyprenyl pathways. 1,4-dihydroxy-2-naphthoyl-CoA synthase (MenB) is the key enzyme for the formation of DHNA. About 2% of the DHNA pool can be transformed into ACNQ through a chemical reaction with NH_3, and the remaining 98% is converted into DMK by 1,4-dihydroxy-2-naphthoate heptaprenyltransferase (MenA). DMK can further be metabolized into menaquinone (MK), which is important in aerobic respiration, by demethylmenaquinone methyltransferase (UbiE) (Conley & Gralnick, 2019; Mevers et al., 2019). We determined the standard redox potential (E^0) of ACNQ and ferricyanide in GM17 to be close to −0.26 and 0.24 V vs. Ag/AgCl, respectively (Figure 4B,C), thus thermodynamically ACNQ should be able to transfer electrons to ferricyanide. To verify this proposed EET pathway (Figure 4A), we knocked out the genes encoding NoxAB, MenA, and MenB. The resulting mutants were named CS4363-NAB, CS4363-MA, and CS4363-MB.

When *menA* was knocked out in CS4363, this resulted in faster growth in ferricyanide supplemented GM17, and CS4363-MA grew with a specific growth rate of 0.741 ± 0.027 h^{-1}, approximately 18% faster than CS4363 in the presence of 150 mM ferricyanide, whereas the final cell density remained the same (Figure 5B(i)). Likewise, the CS4363-MA acidified the medium more quickly than CS4363 (Figure 5B(ii)) and the glucose consumption rate was higher than for CS4363 (Figure 5B(iii)). In contrast, when *menB* was knocked out, formation of DHNA, and thus of ACNQ, was prevented, and this almost completely eliminated EET. An interesting observation was that CS4363-MB grew slightly better than CS4363 without ferricyanide, which indicated that other compounds besides ACNQ could serve as electron carrier. When the NADH dehydrogenase was eliminated, this also eliminated EET. In the presence of ferricyanide, CS4363-NAB displayed the same poor growth as CS4363 in the absence of ferricyanide, demonstrating that the NADH dehydrogenase (NoxAB) is an essential component for EET in

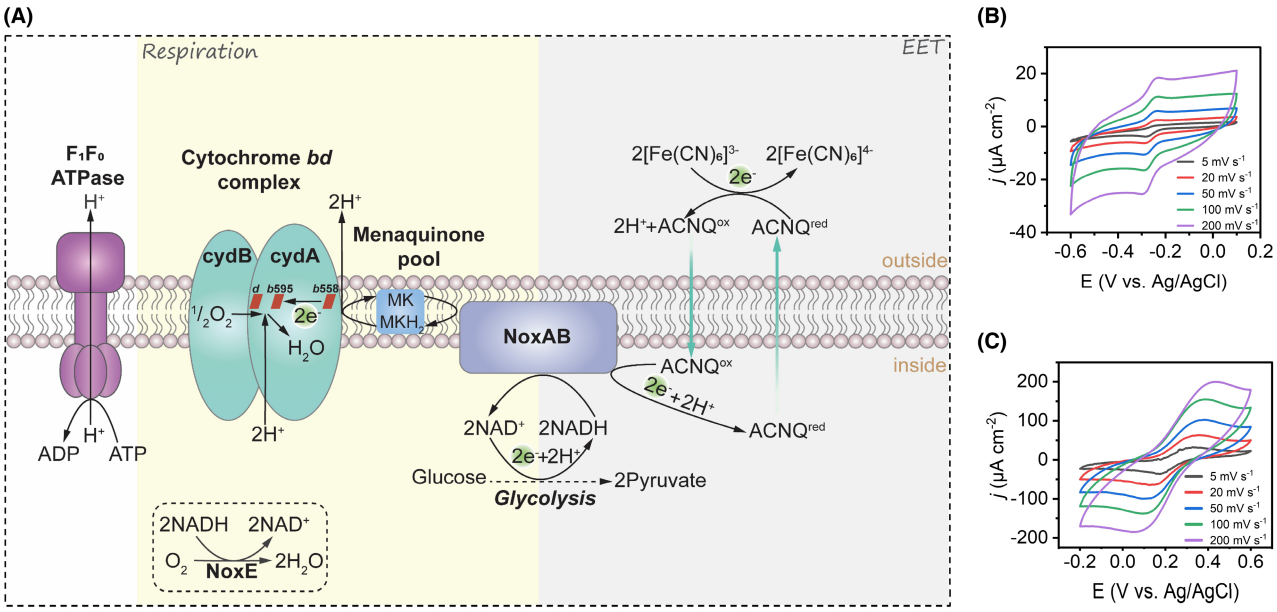

FIGURE 4 Schematic drawing of pathway for NAD^+ regeneration and cyclic voltamograms (CVs). (A) Respiration and proposed mechanism of ACNQ-mediated ferricyanide reduction. NoxAB: NADH dehydrogenase; NoxE: NADH oxidase; F_1F_0-ATPase: F_1F_0-ATP synthase; MK: menaquinone; MKH_2: menaquinol. CVs of 0.023 mM ACNQ (B), 1 mM ferricyanide (C) at different scan rates.

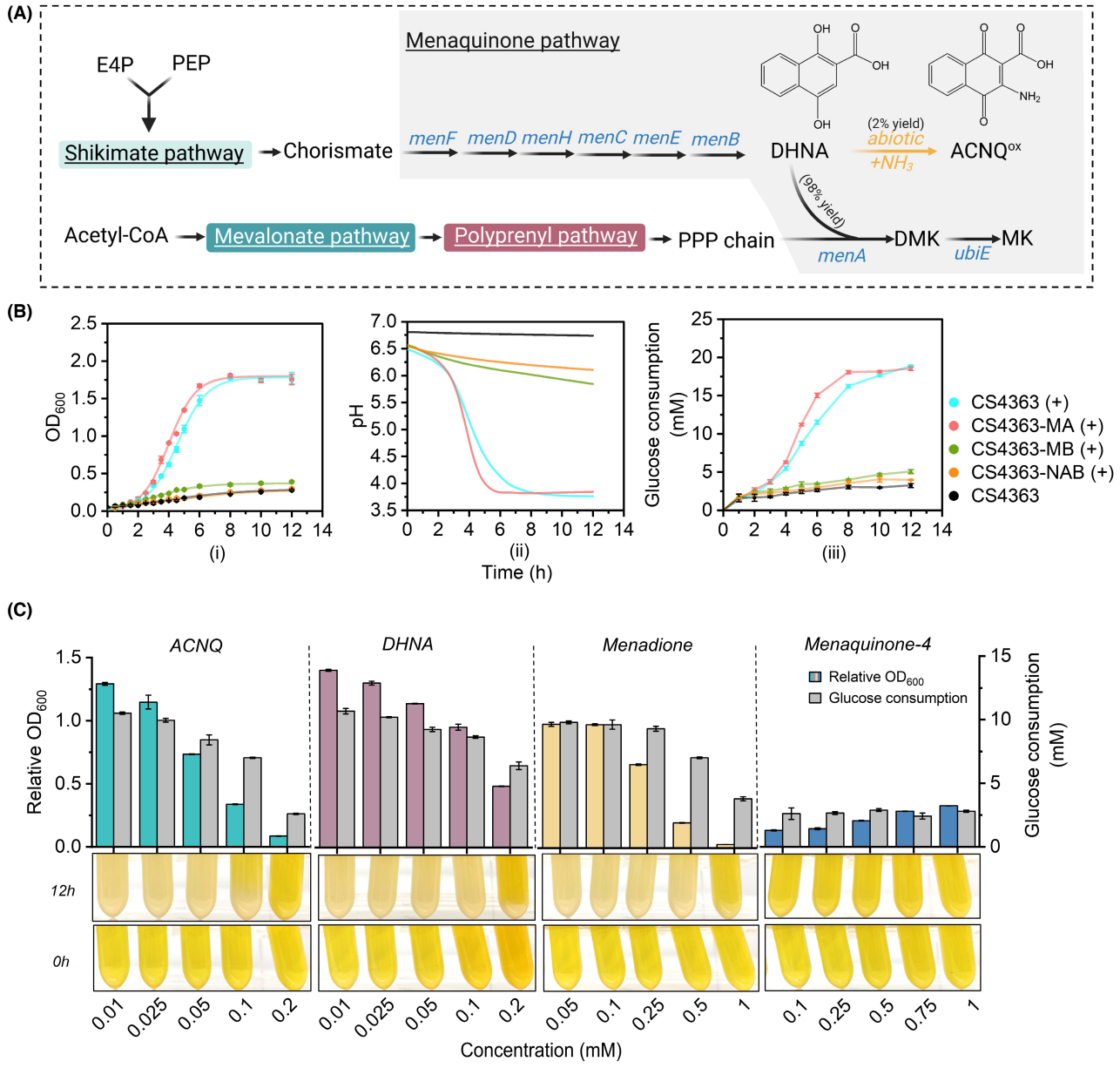

FIGURE 5 The involvement of NADH dehydrogenas and quinones in EET. (A) The quinone biosynthesis pathway in *L. lactis*. MenF: isochorismate synthase; MenD: 2-succinyl-5-enolpyruvyl-6-hydroxy-3-cyclohexene-1-carboxylate synthase; MenH: demethylmenaquinone methyltransferase; MenC: o-succinylbenzoate synthase; MenE: o-succinylbenzoate-CoA ligase; MenB: 1,4-dihydroxy-2-naphthoyl-CoA synthase; MenA: 1,4-dihydroxy-2-naphthoate heptaprenyltransferase; UbiE: demethylmenaquinone methyltransferase; PEP: phosphoenolpyruvate; E4P: D-erythrose-4-phosphate; PPP: polyprenyl diphosphate; DHNA: 1,4-dihydroxy-2-naphthoate; ACNQ: 2-amino-3-carboxy-l,4-naphthoquinone; DMK: demethylmenaquinone; MK: menaquinone. (B) The growth curve (i), pH change with time (ii) and glucose consumption change with time (iii) of CS4363 and knock-out strains with 150 mM ferricyanide. (+) indicates the addition of 150 mM ferricyanide. (C) The relative OD_{600} and glucose consumption of CS4363-MB with different concentrations of ACNQ, DHNA, DMK analogue menadione, and MK-4 with 50 mM ferricyanide. The colour change at 0 and 12 h (the bottom row). The relative OD_{600} = OD_{600} (add ACNQ/DHNA/menadione/MK-4) – OD_{600} (add same volume of methanol/ethanol) was presented. CS4363 and knock-out strains were cultured in GM17 supplemented with ferricyanide under relative anaerobic condition.

L. lactis when using ferricyanide as the terminal electron acceptor.

The *menB* knock-out strain CS4363-MB was then used in complementation studies where the growth stimulatory effect of different quinones was investigated. As shown in Figure 5C, supplementation with ACNQ, DHNA, and the DMK analogue menadione was able to restore growth of CS4363-MB, whereas MK-4 failed to do this. The growth stimulatory effect could also be observed on agar plates when CS4363-MB was streaked in close proximity to CS4363 or CS4363-MA (Figure S2), and thus growth stimulating quinones are released to the surroundings by LAB able to synthesize DHNA. Even though the EET ability of CS4363-MB

could be restored by adding DHNA (Figure 5C), we were unable to detect DHNA in the culture medium of CS4363-MB, whereas ACNQ was detected after 12 h and the yield was around 2%, which is consistent with previous findings (Figure S3). It has been stated that menadione (Vitamin K_3) can serve the same function as DMK (Pankratova et al., 2018). Menadione has a suitably low E^0 (−0.18 V vs. Ag/AgCl, Figure S4A), thus enabling it to serve as an electron mediator to ferricyanide, and this compound was also able to restore the EET ability of CS4363-MB. In an attempt to achieve build-up of DMK, which may be able to participate in EET and thus stimulate growth, the gene *ubiE*, coding for the enzyme that converts DMK into MK, was knocked out. The resulting strain CS4363-UE, however, did not grow better than CS4363 in the presence of 150 mM ferricyanide (Figure S4B–D). These results clearly show that NoxAB and ACNQ are key components of EET when ferricyanide is used as the final electron acceptor.

Using adaptive laboratory evolution to enhance extracellular electron transfer capacity of *L. lactis*

The growth stimulatory effect of ferricyanide on CS4363 was found to be directly correlated with the concentration of ferricyanide (Figure 2A). To improve the capacity for EET of *L. lactis* at lower concentrations of ferricyanide, CS4363 was adaptively evolved in the presence of 50 mM ferricyanide anaerobically. The rationale was that faster-growing mutants might be better at doing EET. After around 300 generations of growth, the faster-growing isolate CS4363-F1 was obtained, which had a specific growth rate of $0.744 \pm 0.002\ h^{-1}$ as compared to $0.419 \pm 0.006\ h^{-1}$ for CS4363 (Figure 6A). Where the main fermentation product of CS4363 was acetoin, CS4363-F1 almost exclusively produced 2,3-butanediol (Figure 6B). The enzyme 2,3-butanediol dehydrogenase (ButBA) catalyses the reduction of acetoin into 2,3-butanediol, a process which consumes NADH, and thus helps regenerate NAD^+ (Figure 1A). The adaptation was continued for an additional 300 generations, which resulted in CS4363-F2, which grew even faster ($\mu_{max} = 0.896 \pm 0.020\ h^{-1}$). CS4363-F1 and CS4363-F2 reached the same high cell density, OD_{600} of 2.8 (Figure 6A). Where CS4363 and CS4363-F1 both accumulated small amounts of pyruvate, CS4363-F2 produced less (0.674 ± 0.077 mM for CS4363-F2 as compared to 2.628 ± 0.189 mM for CS4363-F1).

In addition to CS4363, a derivative lacking NADH oxidase and 2,3-butanediol dehydrogenase, AceN, was adapted as well (Figure 6C). AceN is only able to grow under aerobic conditions when respiration is active, i.e. in the presence of hemin or another heme source (Liu et al., 2017). Interestingly, the adapted derivate AceN-F could not grow aerobically with 2.5 μg/mL hemin after around 3 months of ALE (Figure 6D), i.e. AceN-F had lost the ability to respire. The colour change observed when ferricyanide is reduced to ferrocyanide, occurred more quickly for AceN-F than its

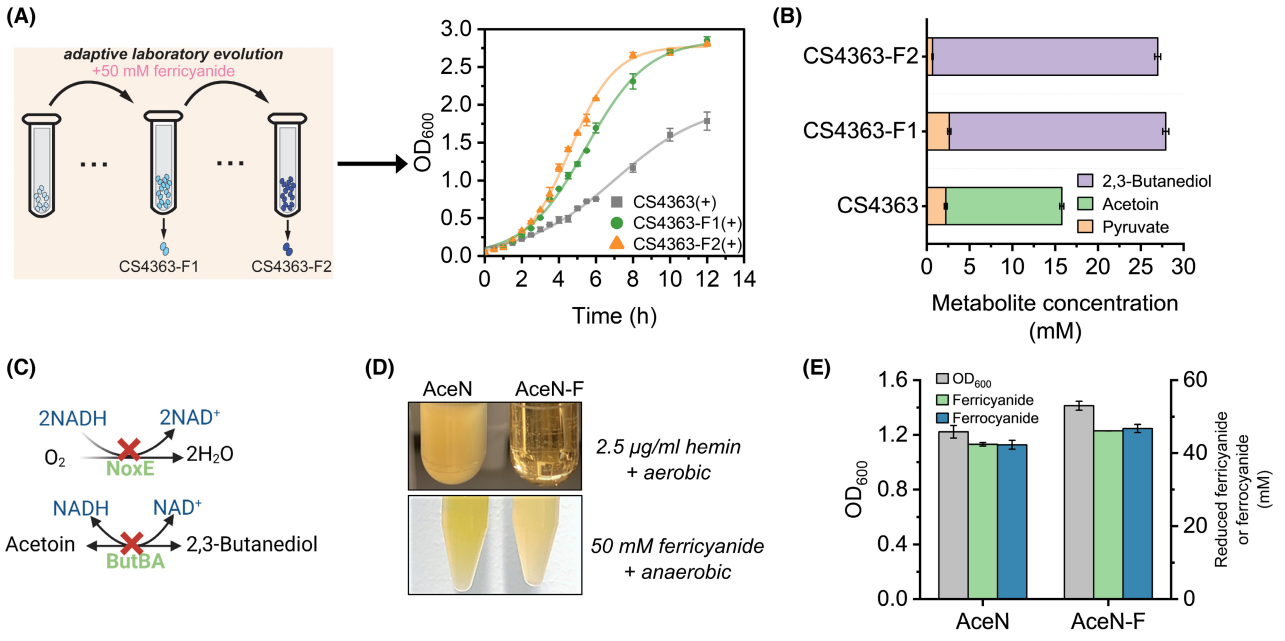

FIGURE 6 The performance of wild-type strains and ALE strains. (A) Illustration of adaptive laboratory evolution under 50 mM ferricyanide (left). Growth performance of CS4363, CS4363-F1, and CS4363-F2 with 50 mM ferricyanide (right). (B) Metabolite compositions of CS4363, CS4363-F1, and CS4363-F2 with 50 mM ferricyanide at 12 h. (+) indicates the addition of 50 mM ferricyanide. (C) Two pathways for NAD^+ regeneration were blocked in AceN. (D) The observed difference between AceN and AceN-F under respiration and EET condition. (E) OD_{600}, ferricyanide reduction and ferrocyanide formation by strains AceN and AceN-F under 50 mM ferricyanide at 16 h.

parent AceN (Figure 6D), and more ferrocyanide was able to accumulate; the AceN-F culture accumulated 46.874 ± 1.127 mM ferrocyanide, while the AceN culture accumulated 42.289 ± 1.242 mM ferrocyanide. The final cell density (OD_{600}) for AceN-F was higher (1.413 ± 0.033) than for AceN (Figure 6E).

Scrutinizing the genomes of the ferricyanide-adapted strains

To determine the underlying reason for (i) the faster growth of the adapted mutants derived from CS4363, and (ii) the lost ability of the adapted AceN mutant to respire, these mutants and their parent strains were sequenced. In CS4363-F1, the insertion sequence IS*905*, the smallest transposable element found in *L. lactis* (Vandecraen et al., 2017), had integrated into the initial coding region of the gene *mlep* and into the region between gene *butB* and *rodA* (Figure 7A). Interestingly, the mapped reads corresponding to the region flanked by these two IS*905* elements were elevated 20-fold as compared to other genes in the genome, indicating the presence of many copies. The *butBA* operon, encoding 2,3-butanediol dehydrogenases, located to this region. For the mutant CS4363-F2, IS*905* had also inserted itself in the coding region of gene *menA* (the start codon ATG + 99 bp), leading to premature termination and thus inactivation of *menA* (Figure 7B). In addition, a single-nucleotide variation (SNV) was found between genes *noxB* and *noxA*, encoding the NADH dehydrogenase (NoxAB), 73 bp upstream of the *noxB* start codon, resulting in an A to C nucleotide change (Figure 7B). By using the online promoter prediction tool BDGP (https://www.fruitfly.org/seq_tools/promoter.html), the promoter sequence of *noxB* was predicted (Table S2) and this SNV located to this promoter, probably altering the expression of *noxB*.

As shown in Figure 7C, in mutant AceN-F, six SNVs were detected in the coding region of *menA*, in the middle of the gene, which most likely caused the inactivation of *menA*. Thus, both in CS4363-F2 and AceN-F, *menA* had been inactivated, leading to an enhanced capacity to respire with ferricyanide, something which was also observed for the engineered CS4363-MA mutant. As mentioned AceN normally depends on hemin-enabled oxygen respiration, since all other NAD^+ regenerating pathways have been eliminated. The loss of this ability concurred with the loss of a functional MenA activity. In addition to these SNVs, AceN-F contained three additional SNV's, one in *copR* encoding a copper-responsive repressor (C-A), one in *purA* encoding adenylosuccinate synthase (C-A) and the final one in upstream of *arcA* encoding arginine deiminase (T-C). The SNV in gene *copR* resulted in an amino acid change from glutamic acid (GAA) to the stop codon (UAA), while the SNV in gene *purA* lead to the amino acid change from cysteine (UGC) to phenylalanine (UUC). The SNV in upstream of *arcA* was also found in the predicted promoter sequence (Table S2).

DISCUSSION

Ferricyanide has different effects on wild-type strain MG1363 and mutant CS4363

Ferricyanide was found to slightly inhibit the growth of the wild-type strain MG1363, and this most likely can be attributed to the toxicity of ferricyanide (Liu et al., 2009). We found that the metabolic flux of MG1363 was redirected in the presence of ferricyanide, and that this was due to EET to ferricyanide. These findings are in good agreement with previous research, although we found slightly different effects on fermentation product composition (Yamazaki et al., 2002).

We also characterized the effect of ferricyanide on *L. lactis* CS4363, which is impaired in NAD^+ regeneration. We found that ferricyanide enabled excellent growth of CS4363, and the growth stimulating effect was found to increase with ferricyanide concentration. As CS4363 lacks LDH, PTA, and ADHE activities (Figure 1A) (Solem et al., 2013), this strain generally requires aeration to grow and mainly forms acetoin and small amounts of pyruvate as its end products. Despite having genes encoding functional 2,3-butanediol dehydrogenases (*butBA*), these are usually not expressed sufficiently to allow for 2,3-butanediol to be formed. In the presence of ferricyanide, acetoin and pyruvate indeed were the main metabolic products formed by CS4363. The NADH generated by glycolysis could be re-oxidized to NAD^+ through EET and the effect of ferricyanide on growth of CS4363 correlated nicely with the NADH/NAD^+ ratio measured, which is similar to the performance of another respiration-dependent strain described in our previous research (Liu et al., 2016). The importance of rapid quenching for obtaining reliable values for intracellular metabolites has often been stressed (Bolten et al., 2007). Here, we relied on a simple approach, where the culture was cooled down and centrifuged at 4°C, after which the cell pellets were frozen rapidly using liquid nitrogen. Although more rapid quenching is possible by using other approaches, we managed to clearly demonstrate the effect of ferricyanide respiration on the NADH/NAD^+ ratio.

We observed that the pH dropped along with cell growth, which at first may appear puzzling as CS4363 lacks a functional lactate dehydrogenase. However, when ferricyanide serves as the final electron acceptor, two protons and two electrons formed are transferred from the quinone pool to the outside,

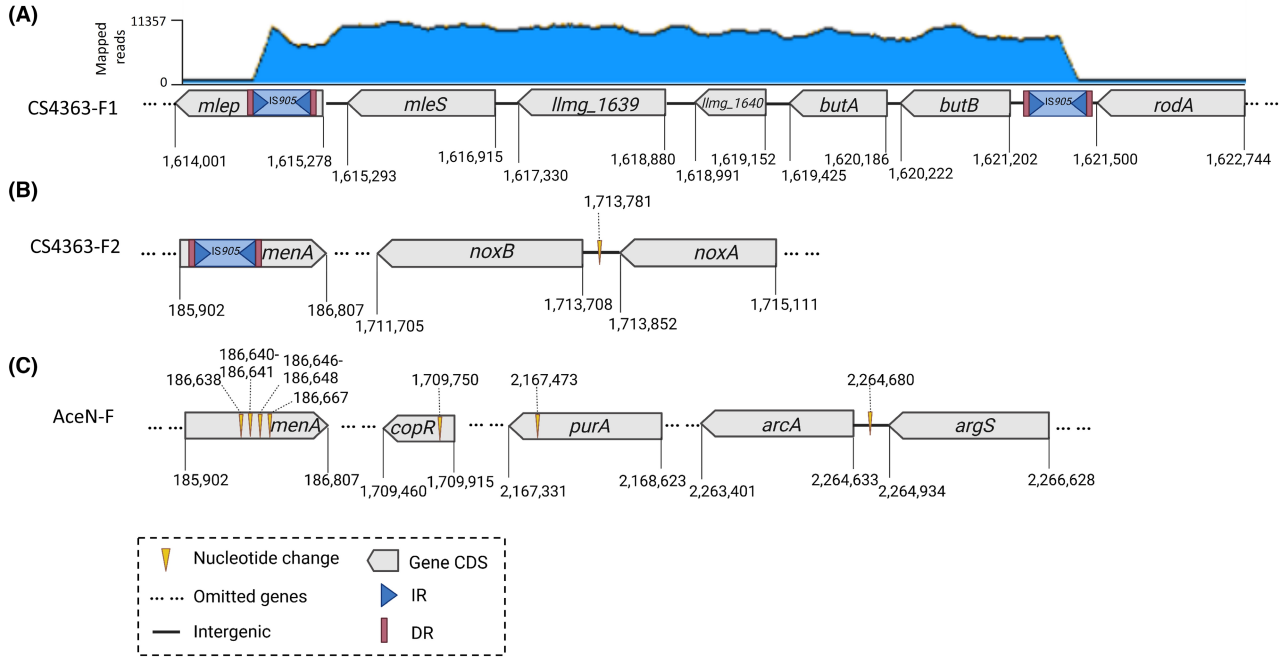

FIGURE 7 Mutations identified in the ferricyanide-adapted mutants. (A) CS4363-F1, (B) CS4363-F2 and (C) AceN-F. Yellow triangle: nucleotide change; Dotted line: omitted genes; Bold line: intergenic; Pentagram: protein coding sequence (CDS) region of the gene; Blue triangle: short terminal inverted repeats (IR); Pink rectangle: directed repeats (DR). IS, insertion sequence. The number on the top of gene CDS: the location of the mutation in the gene. The number on the bottom of gene CDS: the location of the gene.

and where the electrons are used to reduce ferricyanide to ferrocyanide, the protons will cause acidification of the fermentation medium. In general, growth of *L. lactis* is greatly hampered when the pH is below 5.0 (Harvey, 1965). The wild-type strain MG1363 normally lowers the pH of the growth medium to around 4.3, but in our case, when CS4363 grew in the presence of ferricyanide, the culture attained a pH as low as 3.72, which has never been reported for *L. lactis*. This enhanced acid tolerance, might be attributed to the changes in cell morphology observed; in the presence of ferricyanide, the cells became enlarged, thereby reducing the surface area-to-volume ratio, which might help the cells to cope with a low extracellular pH, by reducing overall influx of protons (Neumann et al., 2005). The cell wall of Gram-positive bacteria consists of peptidoglycan (PG) which is decorated with teichoic acids (TAs), polysaccharides (PSs), and proteins (Chapot-Chartier & Kulakauskas, 2014). PG provides strength and rigidity to the cell wall and maintains cell shape (Deghorain et al., 2010). The cell wall can serve as a reservoir of H^+ (Calamita et al., 2001; Kemper et al., 1993), and since ferricyanide respiration generates protons, this may result in the breaking of bonds in the PG, thereby reducing the stiffness of the cell wall, enabling it to stretch and expand (Wheeler et al., 2015), ultimately resulting in the cell morphology we observe for CS4363 in the presence of ferricyanide. Further work is needed to verify this hypothesis.

ACNQ and NoxAB are essential for EET with ferricyanide as the final electron acceptor

In our case, inactivation of the *noxAB* genes in CS4363 resulted in poor growth with ferricyanide, similar to that observed for CS4363 grown without ferricyanide. This was somewhat expected, as NoxAB is the most likely candidate for transferring electrons and protons from NADH to ACNQ. Due to its biphasic partition properties and ability to diffuse rapidly, ACNQ can serve as an electron shuttle inside and outside cells (Mevers et al., 2019; Newman & Kolter, 2000; Yamazaki et al., 1998), and the reduced ACNQ can subsequently be reoxidized by ferricyanide in a non-enzymatic manner. The permeability of the cytoplasmic membrane to ferricyanide is low due to its large negative charge (Löw et al., 1985), and thus ferricyanide is reduced outside the cells.

Inactivation of *menA* in CS4363 surprisingly improved its growth rate, and this appeared to be due to accumulation of DHNA or ACNQ, which enhanced the capacity for EET to ferricyanide. It was possible to restore growth of a *menB* mutant of CS4363 by adding either DHNA, ACNQ, or the DMK analogue menadione to the medium, confirming the involvement of these quinone compounds in EET. However, MK-4 was not involved in EET of the *menB* mutant of CS4363. Furthermore, it was demonstrated that both CS4363, and in particular its *menA* mutant could enable growth of *menB* mutant, when grown together

on solid medium. Since only ACNQ, and not DHNA, could be detected in the culture medium of the *menB* mutant supplemented with DHNA, this substantiates that ACNQ indeed is the main involved quinone in EET.

The DMK analogue menadione can function in EET to ferricyanide

We found that the DMK analogue menadione also could restore the growth of a *menB* mutant of CS4363. This is compatible with menadione having a much lower E^0 than ferricyanide, low enough for it to serve as an electron carrier to ferricyanide. Since the DMK analogue menadione supported EET to ferricyanide, we decided to try and enhance the DMK pool by knocking out *ubiE*, which encodes an enzyme transforming DMK into MK. However, the resulting strain did not display an improved EET ability. This lack of stimulation could be due to menadione having a different structure from DMK (Rezaïki et al., 2008), as menadione lacks the isoprenoid chain and is probably less hydrophobic enabling it to function like ACNQ (Koley & Bard, 2012; Yashiki & Yamashoji, 1996). Although menadione enabled the *menB* mutant to grow, this compound is far less efficient at facilitating EET. Yamazaki et al. mentioned that menadione was approximately 1000 times less efficient at stimulating growth of bifidobacteria than ACNQ (Yamazaki et al., 1998).

Ferricyanide adaptation enhances EET capacity and proves the key role of gene *menA*

To help find the underlying cause for the observed enhanced EET ability, we conducted full genome sequencing. In the initial 300-generation ALE of CS4363, production of 2,3-butanediol increased drastically due to massive amplification on the chromosome of a gene fragment containing the *butBA* operon. Genome sequencing revealed that this was caused by insertion of two IS*905s*, which flanked the gene fragment. The two IS*905s* appeared to have generated a composite replicative transposon, which subsequently had replicated itself several times, inserting copies at new sites (Chandler, 1998). Mutations in gene *menA* were found in both CS4363-F2 and AceN-F. The difference was that one was caused by insertion of IS*905* and another was caused by six SNVs closed to the C-terminal of *menA*. Combined with the previous results in this work, the inactivation of *menA* can enhance the EET ability. Here the mutations in *menA* after ALE in both strains were found to cause inactivation. The lack of *menA* resulted in the lack of MK, which explained why AceN-F had lost the ability to respire. Another mutation was found in *copR*, which encodes a CopY-type repressor can tightly regulate the copper homeostasis to preclude toxic effects (Abicht et al., 2013). MK can accentuate the toxic effect of copper, by facilitating copper reduction (Abicht et al., 2013). The mutation in *copR* probably is not beneficial for EET, however, most likely does not confer any disadvantages to strains unable to generate MK. In CS4363-F2, the mutation in the promoter sequence of gene *noxB* may increase expression, which could be another reason for its improved EET ability. In AceN-F, the overexpression of adenylosuccinate synthase encoded by gene *purA* was recently shown to favour adenine nucleotide synthesis (Dorau et al., 2021), which can promote the formation of ATP (Kilstrup et al., 2005). The amino acid change in *purA* may increase the activity of the encoded enzyme and further improve the energy formation in AceN-F. Arginine deiminase (ADI) encoded by gene *arcA* is the first enzyme in the ADI pathway. The ADI pathway renders one molecule of ATP and consumes two H^+, which contributes to the internal pH homeostasis and opposes external acid stress (Díez et al., 2017). The SNV in the promoter sequence of *arcA* may promote the expression of ADI and thereby help cells to maintain internal pH homeostasis.

CONCLUSION

To the best of our knowledge, this is the first study describing the effect of EET on growth of *L. lactis* and the use of ALE to improve EET capacity. The main mechanism behind EET was elucidated and it was found that the capacity for EET could be enhanced by rendering *menA* inactive. ACNQ mediated EET appears to be the main type of EET in operation in *L. lactis*, however, other EET mechanisms seem to be functional, albeit at low level, and these need to be further explored (Light et al., 2018; Masuda et al., 2010). For sustainable food applications, the toxic ferricyanide should be replaced with other harmless electron acceptors (with a similar redox potential and insensitive to dioxygen) or electrodes. In the future, there are many promising applications of EET, e.g., it could help avoid the oxidative stress frequently imposed on microorganisms during aerated culturing, and EET could serve as an alternative to costly aerated cultivation of microorganisms. Furthermore, EET can be used to redirect metabolic fluxes, by altering $NADH/NAD^+$, instead of using genetic engineering/mutagenesis to knock out NAD^+-regenerating pathways. The preliminary exploration carried out here can lay the foundation for future applications of the electro-fermentation technology. It is possible that harvesting of electricity and production of food ingredients can be accomplished simultaneously by using this promising technology.

AUTHOR CONTRIBUTIONS

Liuyan Gu: Data curation (lead); formal analysis (lead); methodology (lead); software (lead); validation (lead); visualization (lead); writing – original draft (lead); writing – review and editing (lead). **Xinxin Xiao:** Data curation (supporting); methodology (equal); software (equal); writing – review and editing (equal). **Ge Zhao:** Data curation (supporting); formal analysis (supporting); methodology (supporting); software (equal). **Kempen Paul:** Data curation (supporting); methodology (supporting). **Shuangqing Zhao:** Conceptualization (supporting); formal analysis (supporting); methodology (supporting). **Jianming Liu:** Methodology (supporting); project administration (supporting); supervision (supporting); writing – review and editing (supporting). **Sang Yup Lee:** Funding acquisition (equal); project administration (equal); supervision (equal); writing – review and editing (equal). **Christian Solem:** Conceptualization (supporting); funding acquisition (lead); methodology (supporting); project administration (lead); supervision (lead); writing – review and editing (equal).

ACKNOWLEDGMENTS

This work is funded by an internal PhD scholarship of Technical University of Denmark (DTU).

CONFLICT OF INTEREST STATEMENT

The authors have declared that no competing interests exist.

ORCID

Liuyan Gu https://orcid.org/0000-0003-1816-2967
Xinxin Xiao https://orcid.org/0000-0002-0240-0038
Ge Zhao https://orcid.org/0000-0002-6737-7983
Paul Kempen https://orcid.org/0000-0003-2179-2257
Shuangqing Zhao https://orcid.org/0000-0001-9296-5931
Jianming Liu https://orcid.org/0000-0001-6527-6049
Sang Yup Lee https://orcid.org/0000-0003-0599-3091
Christian Solem https://orcid.org/0000-0002-3898-280X

REFERENCES

Abicht, H.K., Gonskikh, Y., Gerber, S.D. & Solioz, M. (2013) Non-enzymic copper reduction by menaquinone enhances copper toxicity in *Lactococcus lactis* IL1403. *Microbiology*, 159, 1190–1197.

Bolten, C.J., Kiefer, P., Letisse, F., Portais, J.C. & Wittmann, C. (2007) Sampling for metabolome analysis of microorganisms. *Analytical Chemistry*, 79, 3843–3849.

Bourdichon, F., Casaregola, S., Farrokh, C., Frisvad, J.C., Gerds, M.L., Hammes, W.P. et al. (2012) Food fermentations: microorganisms with technological beneficial use. *International Journal of Food Microbiology*, 154, 87–97.

Brooijmans, R.J.W., Poolman, B., Schuurman-Wolters, G., de Vos, W.M. & Hugenholtz, J. (2007) Generation of a membrane potential by *Lactococcus lactis* through aerobic electron transport. *Journal of Bacteriology*, 189, 5203–5209.

Calamita, H.G., Ehringer, W.D., Koch, A.L. & Doyle, R.J. (2001) Evidence that the cell wall of *Bacillus subtilis* is protonated during respiration. *Proceedings of the National Academy of Sciences of the United States of America*, 98, 15260–15263.

Chandler, M.S. (1998) Insertion sequences and transposons BT. In: de Bruijn, F.J., Lupski, J.R. & Weinstock, G.M. (Eds.) *Bacterial genomes: physical structure and analysis*. Boston, MA: Springer US, pp. 30–37.

Chapot-Chartier, M.P. & Kulakauskas, S. (2014) Cell wall structure and function in lactic acid bacteria. *Microbial Cell Factories*, 13, 1–23.

Collins, J., Zhang, T., Huston, S., Sun, F., Percival Zhang, Y.H. & Fu, J. (2016) A hidden transhydrogen activity of a FMN-bound diaphorase under anaerobic conditions. *PLoS ONE*, 11, 1–9.

Conley, B. & Gralnick, J. (2019) Solving a shuttle mystery. *eLife*, 8, e49831.

Deghorain, M., Fontaine, L., David, B., Mainardi, J.L., Courtin, P., Daniel, R. et al. (2010) Functional and morphological adaptation to peptidoglycan precursor alteration in *Lactococcus lactis*. *The Journal of Biological Chemistry*, 285, 24003–24013.

Díez, L., Solopova, A., Fernández-Pérez, R., González, M., Tenorio, C., Kuipers, O.P. et al. (2017) Transcriptome analysis shows activation of the arginine deiminase pathway in *Lactococcus lactis* as a response to ethanol stress. *International Journal of Food Microbiology*, 257, 41–48.

Domingo, P.L., Garcia, B. & Leal, J.M. (1990) Acid-base behaviour of the ferricyanide ion in perchloric acid media. Spectrophotometric and kinetic study. *Canadian Journal of Chemistry*, 68, 228–235.

Dorau, R., Chen, J., Liu, J., Ruhdal Jensen, P. & Solem, C. (2021) Adaptive laboratory evolution as a means to generate *Lactococcus lactis* strains with improved thermotolerance and ability to autolyze. *Applied and Environmental Microbiology*, 87, e0103521.

Freguia, S., Masuda, M., Tsujimura, S. & Kano, K. (2009) *Lactococcus lactis* catalyses electricity generation at microbial fuel cell anodes via excretion of a soluble quinone. *Bioelectrochemistry*, 76, 14–18.

Harvey, R.J. (1965) Damage to *Streptococcus lactis* resulting from growth at low pH. *Journal of Bacteriology*, 90, 1330–1336.

Hederstedt, L., Gorton, L. & Pankratovab, G. (2020) Two routes for extracellular electron transfer in *Enterococcus faecalis*. *Journal of Bacteriology*, 202, 1–9.

Holo, H. & Nes, I.F. (1989) High-frequency transformation, by electroporation, of *Lactococcus lactis* subsp. *cremoris* grown with glycine in osmotically stabilized media. *Applied and Environmental Microbiology*, 55, 3119–3123.

Hugenholtz, J., Kleerebezem, M., Starrenburg, M., Delcour, J., De Vos, W. & Hols, P. (2000) *Lactococcus lactis* as a cell factory for high-level diacetyl production. *Applied and Environmental Microbiology*, 66, 4112–4114.

Husmann, S., Zarbin, A.J.G. & Dryfe, R.A.W. (2020) High-performance aqueous rechargeable potassium batteries prepared via interfacial synthesis of a Prussian blue-carbon nanotube composite. *Electrochimica Acta*, 349, 136243.

Johnson, D.R. & Decker, E.A. (2015) The role of oxygen in lipid oxidation reactions: a review. *Annual Review of Food Science and Technology*, 6, 171–190.

Kemper, M.A., Urrutia, M.M., Beveridge, T.J., Koch, A.L. & Doyle, R.J. (1993) Proton motive force may regulate cell wall-associated enzymes of *Bacillus subtilis*. *Journal of Bacteriology*, 175, 5690–5696.

Kilstrup, M., Hammer, K., Jensen, P.R. & Martinussen, J. (2005) Nucleotide metabolism and its control in lactic acid bacteria. *FEMS Microbiology Reviews*, 29, 555–590.

Koebmann, B., Blank, L.M., Solem, C., Petranovic, D., Nielsen, L.K. & Jensen, P.R. (2008) Increased biomass yield of *Lactococcus lactis* during energetically limited growth and respiratory conditions. *Biotechnology and Applied Biochemistry*, 50, 25–33.

Koley, D. & Bard, A.J. (2012) Inhibition of the MRP1-mediated transport of the menadione-glutathione conjugate (thiodione) in HeLa cells as studied by SECM. *Proceedings of the National Academy of Sciences of the United States of America*, 109, 11522–11527.

Lai, B., Yu, S., Bernhardt, P.V., Rabaey, K., Virdis, B. & Krömer, J.O. (2016) Anoxic metabolism and biochemical production in *Pseudomonas putida* F1 driven by a bioelectrochemical system. *Biotechnology for Biofuels*, 9, 1–13.

Lam, L.N., Wong, J.J., Matysik, A., Paxman, J.J., Chong, K.K.L., Low, P.M. et al. (2019) Sortase-assembled pili promote extracellular electron transfer and iron acquisition in *Enterococcus faecalis* biofilm. *bioRxiv*, 601666.

Lan, C.Q., Oddone, G., Mills, D.A. & Block, D.E. (2006) Kinetics of *Lactococcus lactis* growth and metabolite formation under aerobic and anaerobic conditions in the presence or absence of hemin. *Biotechnology and Bioengineering*, 95, 1070–1080.

Light, S.H., Su, L., Rivera-Lugo, R., Cornejo, J.A., Louie, A., Iavarone, A.T. et al. (2018) A flavin-based extracellular electron transfer mechanism in diverse gram-positive bacteria. *Nature*, 562, 140–157.

Liu, J., Chan, S.H.J., Brock-Nannestad, T., Chen, J., Lee, S.Y., Solem, C. et al. (2016) Combining metabolic engineering and biocompatible chemistry for high-yield production of homo-diacetyl and homo-(S,S)-2,3-butanediol. *Metabolic Engineering*, 36, 57–67.

Liu, C., Sun, T., Zhai, Y. & Dong, S. (2009) Evaluation of ferricyanide effects on microorganisms with multi-methods. *Talanta*, 78, 613–617.

Liu, J., Wang, Z., Kandasamy, V., Lee, S.Y., Solem, C. & Jensen, P.R. (2017) Harnessing the respiration machinery for high-yield production of chemicals in metabolically engineered *Lactococcus lactis*. *Metabolic Engineering*, 44, 22–29.

Logan, B.E. (2009) Exoelectrogenic bacteria that power microbial fuel cells. *Nature Reviews. Microbiology*, 7, 375–381.

Löw, H., Crane, F.L., Partick, E.J. & Clark, M.G. (1985) α-Adrenergic stimulation of trans-sarcolemma electron efflux in perfused rat heart. Possible regulation of Ca^{2+}-channels by a sarcolemma redox system. *Biochimica et Biophysica Acta*, 844, 142–148.

Masuda, M., Freguia, S., Wang, Y.F., Tsujimura, S. & Kano, K. (2010) Flavins contained in yeast extract are exploited for anodic electron transfer by *Lactococcus lactis*. *Bioelectrochemistry*, 78, 173–175.

Mevers, E., Su, L., Pishchany, G., Baruch, M., Cornejo, J., Hobert, E. et al. (2019) An elusive electron shuttle from a facultative anaerobe. *eLife*, 8, e48054.

Naradasu, D., Miran, W., Sakamoto, M. & Okamoto, A. (2019) Isolation and characterization of human gut bacteria capable of extracellular electron transport by electrochemical techniques. *Frontiers in Microbiology*, 10, 1–9.

Neumann, G., Veeranagouda, Y., Karegoudar, T.B., Sahin, Ö., Mäusezahl, I., Kabelitz, N. et al. (2005) Cells of *Pseudomonas putida* and *Enterobacter* sp. adapt to toxic organic compounds by increasing their size. *Extremophiles*, 9, 163–168.

Newman, D.K. & Kolter, R. (2000) A role for excreted quinones in extracellular electron transfer. *Nature*, 405, 94–97.

Pankratova, G., Leech, D., Gorton, L. & Hederstedt, L. (2018) Extracellular electron transfer by the gram-positive bacterium *Enterococcus faecalis*. *Biochemistry*, 57, 4597–4603.

Pedersen, M.B., Gaudu, P., Lechardeur, D., Petit, M.A. & Gruss, A. (2012) Aerobic respiration metabolism in lactic acid bacteria and uses in biotechnology. *Annual Review of Food Science and Technology*, 3, 37–58.

Rezaïki, L., Cesselin, B., Yamamoto, Y., Vido, K., Van West, E., Gaudu, P. et al. (2004) Respiration metabolism reduces oxidative and acid stress to improve long-term survival of *Lactococcus lactis*. *Molecular Microbiology*, 53, 1331–1342.

Rezaïki, L., Lamberet, G., Derré, A., Gruss, A. & Gaudu, P. (2008) *Lactococcus lactis* produces short-chain quinones that cross-feed group B *streptococcus* to activate respiration growth. *Molecular Microbiology*, 67, 947–957.

Rhoads, A., Beyenal, H. & Lewandowski, Z. (2005) Microbial fuel cell using anaerobic respiration as an anodic reaction and biomineralized manganese as a cathodic reactant. *Environmental Science & Technology*, 39, 4666–4671.

Rodrigues, F., Côrte-Real, M., Leao, C., Van Dijken, J.P. & Pronk, J.T. (2001) Oxygen requirements of the food spoilage yeast *Zygosaccharomyces bailii* in synthetic and complex media. *Applied and Environmental Microbiology*, 67, 2123–2128.

Saunders, S.H. & Newman, D.K. (2018) Extracellular electron transfer transcends microbe-mineral interactions. *Cell Host & Microbe*, 24, 611–613.

Schröder, U., Harnisch, F. & Angenent, L.T. (2015) Microbial electrochemistry and technology: terminology and classification. *Energy & Environmental Science*, 8, 513–519.

Shi, L., Dong, H., Reguera, G., Beyenal, H., Lu, A., Liu, J. et al. (2016) Extracellular electron transfer mechanisms between microorganisms and minerals. *Nature Reviews. Microbiology*, 14, 651–662.

Solem, C., Defoor, E., Jensen, P.R. & Martinussen, J. (2008) Plasmid pCS1966, a new selection/counterselection tool for lactic acid bacterium strain construction based on the oroP gene, encoding an orotate transporter from *Lactococcus lactis*. *Applied and Environmental Microbiology*, 74, 4772–4775.

Solem, C., Dehli, T. & Jensen, P.R. (2013) Rewiring *Lactococcus lactis* for ethanol production. *Applied and Environmental Microbiology*, 79, 2512–2518.

Tejedor-Sanz, S., Stevens, E.T., Finnegan, P., Nelson, J., Knoessen, A., Light, S.H. et al. (2022) Extracellular electron transfer increases fermentation in lactic acid bacteria via a hybrid metabolism. *eLife*, 11, e70684.

Ucar, D., Zhang, Y. & Angelidaki, I. (2017) An overview of electron acceptors in microbial fuel cells. *Frontiers in Microbiology*, 8, 1–14.

Vandecraen, J., Chandler, M., Aertsen, A. & Van Houdt, R. (2017) The impact of insertion sequences on bacterial genome plasticity and adaptability. *Critical Reviews in Microbiology*, 43, 709–730.

Wang, W., Du, Y., Yang, S., Du, X., Li, M., Lin, B. et al. (2019) Bacterial extracellular electron transfer occurs in mammalian gut. *Analytical Chemistry*, 91, 12138–12141.

Wheeler, R., Turner, R.D., Bailey, R.G., Salamaga, B., Mesnage, S., Mohamad, S.A.S. et al. (2015) Bacterial cell enlargement requires control of cell wall stiffness mediated by peptidoglycan hydrolases. *mBio*, 6, 1–10.

Widdel, F. (2010) *Theory and measurement of bacterial growth. A basic and practical aspects*. Bremen: Grundpraktikum Mikrobiologie; University of Bremen.

Yamazaki, S.I., Kaneko, T., Taketomo, N., Kano, K. & Ikeda, T. (2002) Glucose metabolism of lactic acid bacteria changed by quinone-mediated extracellular electron transfer. *Bioscience, Biotechnology, and Biochemistry*, 66, 2100–2106.

Yamazaki, S.I., Kano, K., Ikeda, T., Isawa, K. & Kaneko, T. (1998) Mechanistic study on the roles of a bifidogenetic growth stimulator based on physicochemical characterization. *Biochimica et Biophysica Acta (BBA)-General Subjects*, 1425, 516–526.

Yan, X., Jansen, C.U., Diao, F., Qvortrup, K., Tanner, D., Ulstrup, J. et al. (2021) Surface-confined redox-active monolayers of a multifunctional anthraquinone derivative on nanoporous and single-crystal gold electrodes. *Electrochemistry Communications*, 124, 106962.

Yashiki, Y. & Yamashoji, S. (1996) Extracellular reduction of menadione and ferricyanide in yeast cell suspension. *Journal of Fermentation and Bioengineering*, 82, 319–321.

Zhou, Y., Liu, C., Zhou, R., Lu, A., Huang, B., Liu, L. et al. (2019) SEQdata-BEACON: a comprehensive database of sequencing performance and statistical tools for performance evaluation and yield simulation in BGISEQ-500. *BioData Mining*, 12, 1–14.

SUPPORTING INFORMATION

Additional supporting information can be found online in the Supporting Information section at the end of this article.

How to cite this article: Gu, L., Xiao, X., Zhao, G., Kempen, P., Zhao, S., Liu, J. et al. (2023) Rewiring the respiratory pathway of *Lactococcus lactis* to enhance extracellular electron transfer. *Microbial Biotechnology*, 16, 1277–1292. Available from: https://doi.org/10.1111/1751-7915.14229